Proceedings of the Eighteenth International Conference on
Civil, Structural and Environmental Engineering Computing
Edited by: P. Iványi, J. Kruis and B.H.V. Topping
Civil-Comp Conferences, Volume 10, Paper 4.6
Civil-Comp Press, Edinburgh, United Kingdom, 2025
ISSN: 2753-3239, doi: 10.4203/ccc.10.4.6

Design of Spatial Truss Structures Using the Circulatory System-Based Optimization

I. B. Ugur[1] and S. O. Degertekin[2]

[1]Department of Civil Engineering, Şırnak University, Turkiye
[2]Department of Civil Engineering, Dicle University, Turkiye

Abstract

Truss structures are widely employed in structural engineering due to their lightweight characteristics, aesthetic appeal, and high structural efficiency. This paper applies the Circulatory System-Based Optimization (CSBO) algorithm. This nature-inspired metaheuristic mimics the human circulatory system's mechanisms for nutrient distribution and waste removal, to the optimal design of a complex spatial truss structure. The selected benchmark problem consists of 198 members and 211 design variables, covering both sizing and shape optimization. The design process accounts for practical structural constraints, including stress, displacement, buckling, and slenderness ratio limitations, as outlined in AISC-LRFD provisions. CSBO is utilized to minimize the structural weight while ensuring full compliance with all design requirements. The results confirm that CSBO exhibits promising performance in terms of convergence stability, solution quality, and effective weight reduction for this challenging high-dimensional truss optimization problem.

Keywords: circulatory system-based optimization, truss optimization, optimum design, structural optimization, metaheuristics, spatial truss.

1 Introduction

Nature has long been a source of inspiration for solving complex optimization problems. In recent decades, numerous metaheuristic algorithms inspired by physical processes, biological evolution, and social dynamics have been developed to address

challenging engineering design tasks. Metaheuristic algorithms such as Genetic Algorithms (GA), Simulated Annealing (SA), Particle Swarm Optimization (PSO), Harmony Search (HS), Big Bang–Big Crunch (BB-BC), Ant Colony Optimization (ACO), Artificial Bee Colony (ABC), Differential Evolution (DE), Gray Wolf Optimizer (GWO), Dandelion Optimizer (DO), Bonobo Optimizer (BO), and Circulatory System-Based Optimization (CSBO) [1-12] have emerged as powerful tools for global optimization. These techniques have been extensively tested in the context of structural optimization, particularly for skeletal systems, as highlighted in various studies [13].

In structural engineering, optimizing shape and size variables remains a challenging yet crucial task. Traditional methods often fall short in tackling the nonlinearity and multimodality inherent in such problems. As a result, metaheuristic algorithms have become a practical and effective alternative for structural designers. Truss structures, widely used for their efficiency and versatility, are prime examples where optimization can lead to significant material savings and enhanced structural performance. However, finding optimal truss designs is far from straightforward. Engineers must navigate a delicate balance between minimizing weight and satisfying strict design constraints, such as stress, displacement, buckling, and slenderness limits.

Numerous metaheuristic techniques have been successfully applied to truss optimization problems, considering both geometric complexity and varying constraints [14-17]. These methods are particularly attractive due to their flexibility and ability to explore complex solution spaces without requiring gradient information. Consequently, they offer significant potential for solving large-scale, high-dimensional optimization problems in structural engineering.

Among these bio-inspired approaches, the Circulatory System-Based Optimization algorithm [12] (CSBO) stands out by simulating the nutrient transport and waste removal processes of the human circulatory system. This unique mechanism enables the algorithm to efficiently explore the design space and avoid premature convergence, making it well-suited for challenging optimization tasks. In this paper, the CSBO algorithm is employed for the optimal design of a highly complex spatial truss structure comprising 198 members and 211 design variables.
The optimization goal is to minimize the total structural weight while strictly adhering to realistic design constraints, including stress, displacement, buckling, and slenderness criteria in accordance with AISC-LRFD provisions. This paper demonstrates the effectiveness of the algorithm in simultaneously optimizing shape and size variables under specified design conditions. Finally, the optimized solution is verified using SAP2000 structural analysis software, providing practical validation of the results.

By focusing on a realistic and complex truss system, this research highlights the capability of CSBO to address sophisticated structural optimization problems, and it reinforces its potential as a valuable tool in civil engineering design optimization.

2 Mathematical Formulations of the Spatial Steel Truss Optimization Problem

The primary goal of structural optimization is to determine the most efficient design that minimizes the structural weight while satisfying all required constraints. In the case of steel trusses, this optimization process typically involves both sizing and layout variables, which together define the design problem. The truss problem can be expressed as follows:

$$W(A,X) = \sum_{k=1}^{N_m} \gamma_k \cdot A_k \cdot L_k \tag{1}$$

$$L_k = \sqrt{(x_{ki} - x_{kj})^2 + (y_{ki} - y_{kj})^2 + (z_{ki} - z_{kj})^2} \tag{2}$$

$$\sigma_k^{c,lim} \leq \sigma_k \leq \sigma_k^{t,lim} \tag{3}$$

$$\delta_{min} < \delta_j < \delta_{max} \tag{4}$$

$$A_{min} < A_k < A_{max} \tag{5}$$

$$g_l \leq 0 \qquad l = 1,2,3 \ldots, N_{cr} \tag{6}$$

Let A_k denote the cross-sectional area of element *k,* where *k*=1,2,3,..,N_m, N_m represents the number of structural elements. *W* is the total truss weight and is computed based on material density γ, length of each element *L,* and corresponding cross-sectional area. The length of each element is determined by the nodal coordinates of its two connecting nodes (x_{ki}, y_{ki}, z_{ki} and x_{kj}, y_{kj}, z_{kj}).

Stress constraints, including the axial stresses under tension and compression, denoted by $\sigma_k^{c,lim}$ and $\sigma_k^{t,lim}$ respectively. Additionally, nodal displacements must remain within prescribed bounds, represented by δ_{min} and δ_{max} The design also respects upper and lower bounds on cross-sectional areas, expressed as A_{min} and A_{max}

All constraints are reformulated in normalized form as g_l where *l*=1,2,…, N_{cr} being the total number of constraints. As an illustration, the displacement constraint g_{disp} is evaluated as follows:

$$g_{disp} = \frac{|\delta_i - \delta_{min}|}{\delta_{min}} \; and \; \frac{|\delta_{max} - \delta_i|}{\delta_{max}} \tag{7}$$

To manage design constraints during the optimization process, a penalty function approach is employed. This method converts the constrained optimization problem into an unconstrained one by assigning penalty terms to solutions that violate the constraints. As a result, the optimization process is guided toward feasible regions of the design space. The penalized objective function incorporating these penalties can be expressed as follows:

$$W_p(A,X) = W(A,X) \cdot (1 + \psi)^e \tag{8}$$

where ψ is the sum of total constraint violations, e is the penalty exponent set to 1.

3 Circulatory System-Based Optimization Algorithm (CSBO)

The human circulatory system serves as the biological inspiration for the CSBO algorithm. At the core of this system lies the heart, which plays a vital role in distributing oxygenated blood throughout the body. Blood vessels serve as transport channels, ensuring the efficient delivery of nutrients and the removal of waste. This system operates through two interrelated circuits: the pulmonary circuit, responsible for oxygenating blood in the lungs, and the systemic circuit, which delivers oxygen-rich blood to tissues and organs [12].

The CSBO algorithm emulates this dual-circuit system to improve optimization performance. It mimics the cyclic nature of blood circulation, where less effective solutions are systematically replaced through processes analogous to oxygenation and revitalization. This biological analogy enhances population diversity, prevents premature convergence, and strengthens the overall search capability of the algorithm [12].

-Initialization

The algorithm begins by randomly generating an initial population, where each solution represents a "blood droplet" with a specific position vector in the design space:

$$X_i = X_{min} + rand(1, Dim) \times (X_{max} - X_{min}) \qquad i = 1{:}\, nPop \qquad (9)$$

where $nPop$ is the population size, and *Dim* denotes the number of design variables.

- ***Blood Mass Movement in Veins:***

Each solution (blood mass) moves under the influence of external forces, simulating pressure differences within the veins. The aim is to minimize the objective function while avoiding entrapment in local optima (analogous to clogged arteries). The position update rule is defined as:

$$X_i^{new} = X_i + K_{i1} \times p_i \times (X_i - X_1) + K_{23} \times p_i \times (X_3 - X_2) \qquad (10)$$

$$K_{ij} = \frac{F(X_j) - F(X_i)}{|F(X_j) - F(X_i)| + \varepsilon} = \begin{cases} 1; & if\ F(X_j) < F(X_i) \\ -1; & if\ F(X_j) > F(X_i) \\ 0; & if\ F(X_j) = F(X_i) \end{cases} \qquad (11)$$

K_{ij} indicates movement direction based on fitness differences, *F* denotes the fitness value, p is the displacement magnitude (bounded between 0 and 1), and ε is a small positive number to avoid division by zero. This mechanism enables the solutions to adjust their positions based on both their fitness and that of selected neighbors, ensuring continuous improvement.

- ***Pulmonary Circulation***

In this phase, the weakest individuals in the population—those with the poorest objective function values—are treated as oxygen-depleted blood droplets. These individuals, denoted by NR are symbolically sent to the lungs for oxygenation, which

corresponds to diversification in the search space. Their positions are updated using random perturbations, as follows:

$$X_i^{new} = X_i + \left(\frac{randn}{it}\right) \times randc(1, Dim) \quad i = 1,2, \dots NR \tag{12}$$

where $randn$ is the random number from a normal distribution, *it* represents the current iteration number, $randc$ denotes a random vector from a Cauchy probability distribution.

- ***Systemic Circulation***

Conversely, individuals with better fitness values—symbolizing oxygenated blood—enter the systemic circulation, where their positions are refined to improve exploitation:

$$X_{i,j}^{new} = X_{1,j} + p_i \times \left(X_{3,j} - X_{2,j}\right) \tag{13}$$

$$p_i = \frac{F(X_i) - Fworst}{Fbest - Fworst} \tag{14}$$

where *Fbest* and *Fworst* represent the best and worst objective function values within the current population, this mechanism steers better solutions toward promising regions of the search space while maintaining diversity.

- ***Termination***

The CSBO algorithm continues to iterate through these circulatory phases until a predefined stopping criterion is satisfied, such as reaching the maximum number of iterations or achieving a convergence threshold.

4 Numerical Examples

This paper evaluates the effectiveness of the proposed algorithm in optimizing the sizing and layout of a complex spatial truss structure consisting of 198 members and 211 design variables. The optimization is performed under the AISC-LRFD [18] design provisions, ensuring that all stress, displacement, and buckling constraints are satisfied. To verify the accuracy and structural feasibility of the optimized design, the results are validated through detailed analysis using SAP2000 software [19]. For a robust performance assessment, the algorithm is executed over 20 independent optimization runs, each with a population size of 45. The optimization process is carried out for a maximum of 2000 iterations to ensure thorough exploration of the design space.

4.1 198-Bar Spatial Truss

The truss structure, consisting of 198 members and 52 nodes, is introduced and optimized for the first time in this investigation. Although this model is inspired by the framework presented in ISCSO-2017 by Bright Optimizer [20], it has been fully developed from scratch with a distinct configuration. The entire geometry, including

initial nodal coordinates, layout constraints, and loading conditions, has been redefined in this study, while maintaining compliance with the AISC-LRFD design provisions. In addition to these differences, slenderness ratio constraints—absent in the original ISCSO model—are incorporated here to provide a more realistic and comprehensive assessment of structural performance. The geometry of the truss is illustrated in Figure 1.

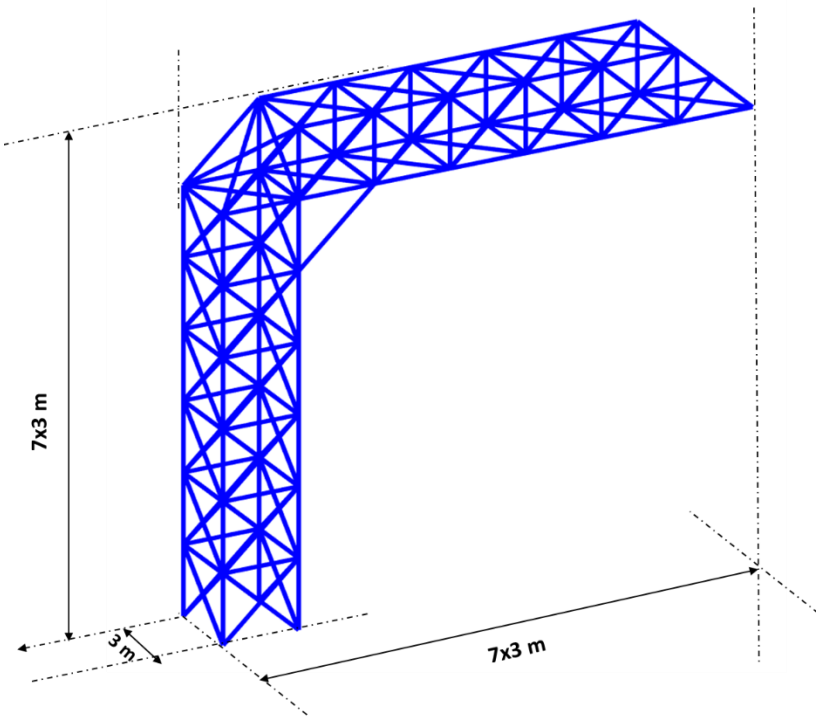

Figure 1: 198-bar spatial truss

The material density, elasticity modulus, and yield stress are considered 7.85 tons/m^3, 200 GPa, and 248.2 MPa, respectively. The truss design is subjected to three independent load cases applying to all unsupported nodes as outlined: (i) 7.5 kN is directed positively along the x-axis, (ii) 7.5 kN is directed positively along the y-axis, and (iii) 10 kN, exerted downward along the negative z-axis.

Since each member of the truss structure is defined as a sizing variable, there are 198 sizing variables in all. Sizing variables are restricted to be chosen from the pipe sections proposed in Table 1. On the other hand, the layout variables comprise a set of 13 shape variables, corresponding to the z-coordinates of the upper nodes and the x-coordinates of the backside nodes of the structure, resulting in a total of 211 design variables.

Sizing variables $\boldsymbol{A} = [A_1; A_2; A_3; \dots A_{198}]_{\mathbf{198\times1}}$

$$Layout\ variables \qquad X = \begin{bmatrix} X_1 = X_2 \\ X_5 = X_6 \\ X_9 = X_{10} \\ X_{13} = X_{14} \\ X_{17} = X_{18} \\ X_{21} = X_{22} \\ X_{25} = X_{26} \\ Z_{41} = Z_{42} \\ Z_{43} = Z_{44} \\ Z_{45} = Z_{46} \\ Z_{47} = Z_{48} \\ Z_{49} = Z_{50} \\ Z_{51} = Z_{52} \end{bmatrix}_{\mathbf{13\times1}}$$

The layout constraints are considered as given below:

$$-9000 \leq X_1, X_5, X_9, X_{13}, X_{17}, X_{21}, X_{25} \leq 2250\ (mm)$$
$$18750 \leq Z_{41}, Z_{43}, Z_{45}, Z_{47}, Z_{49}, Z_{51} \leq 30000\ (mm)$$

According to the AISC-LRFD design code, the member's tensile force must not exceed the tensile strength of the member, as stated below:

$$P_u \geq \phi_t \cdot P_n \tag{20}$$

The ultimate tensile force is denoted as P_u. The resistance factor for tension is represented by ϕ_t, where ϕ_t= 0.9. The nominal tensile strength of the member is indicated as P_n and is calculated as $P_n = A_g \cdot F_y$, with F_y representing the yield stress of the steel.

Conversely, in the design of a member under compressive force, it is essential to ensure that the compressive force does not exceed the compressive strength of the member. This constraint, as per AISC-LRFD standards, can be expressed as follows:

$$P_u \geq \phi_c \cdot P_n \tag{21}$$

where P_u stands for the ultimate member of compressive force. The resistance factor for compression is denoted as ϕ_c, where ϕ_c = 0.85. Similarly, P_n represents the nominal tensile strength of the member, calculated as $P_n = A_g \cdot F_{cr}$. Here, F_{cr} is determined as follows:

$$F_{cr} = \begin{Bmatrix} \left(0.658^{{\lambda_c}^2}\right) \cdot F_y & if\ \lambda_c \leq 1.5 \\ \left[\frac{0.877}{{\lambda_c}^2}\right] \cdot F_y & if\ \lambda_c > 1.5 \end{Bmatrix} \tag{22}$$

where λ_c is calculated using Eq. (23):

$$\lambda_c = max\left\{\left(\frac{K_x L_x}{r_x \pi}\sqrt{\frac{F_y}{E}}\right); \left(\frac{K_y L_y}{r_y \pi}\sqrt{\frac{F_y}{E}}\right)\right\} \tag{23}$$

Here, K_x, L_x, and r_x represent the effective buckling length and the radius of gyration around the *x*-axis, respectively. Similarly, K_y, L_y, and r_y denote the corresponding

values around the *y*-axis. In this paper, effective length factors (K_x, K_y) are considered 1 for truss members.

The slenderness ratio constraints in compression or tension are calculated for each member as follows:

$$\lambda_i = \begin{Bmatrix} \dfrac{K_i L_i}{r_i} \le 300 & for\ tension\ members \\ \dfrac{K_i L_i}{r_i} \le 200 & for\ compression\ members \end{Bmatrix} \quad (24)$$

The displacements of all unsupported nodes are constrained to ±100 mm nodes in the *x, y,* and *z* directions.

No	Pipe Section	Area (mm^2)	Radius of Gyration	No	Pipe Section	Area (mm^2)	Radius of Gyration
1	PIPE1/2Std	161.29	6.6235	19	PIPE4Std	2045.157	38.3595
2	PIPE1/2XS	206.4512	6.35	20	PIPE3-1/2XS	2374.189	33.181
3	PIPE3/4Std	214.8383	8.4667	21	PIPE2-1/2XXS	2599.995	21.4349
4	PIPE3/4XS	279.3543	8.1883	22	PIPE5Std	2774.188	47.7553
5	PIPE1Std	318.709	10.6593	23	PIPE4XS	2845.156	37.4952
6	PIPE1XS	412.2572	10.3451	24	PIPE3XXS	3529.025	26.5799
7	PIPE1-1/4Std	431.6121	13.7132	25	PIPE6Std	3599.993	56.9993
8	PIPE1-1/2Std	515.4829	15.8213	26	PIPE5XS	3941.928	46.7518
9	PIPE1-1/4XS	568.3859	13.3123	27	PIPE4XXS	5225.796	34.909
10	PIPE2Std	690.3212	20.0391	28	PIPE8Std	5419.344	74.6213
11	PIPE1-1/2XS	690.3212	15.3543	29	PIPE6XS	5419.344	55.7727
12	PIPE2XS	954.8368	19.4519	30	PIPE5XXS	7290.308	43.799
13	PIPE2-1/2Std	1096.772	24.0966	31	PIPE10Std	7677.404	93.4272
14	PIPE3Std	1438.707	29.5587	32	PIPE8XS	8258.048	73.094
15	PIPE2-1/2XS	1451.61	23.4635	33	PIPE12Std	9419.336	111.0349
16	PIPE2XXS	1716.126	17.825	34	PIPE6XXS	10064.5	52.3634
17	PIPE3-1/2Std	1729.029	33.9574	35	PIPE10XS	10387.08	92.1698
18	PIPE3XS	1948.383	28.8274	36	PIPE12XS	12387.07	110.2903
				37	PIPE8XXS	13741.91	70.0489

Table 1: Pipe section list for 198-bar spatial truss

The optimization results for the 198-bar spatial truss, summarized in Table 2, demonstrate the effectiveness and robustness of the CSBO algorithm. The best solution obtained corresponds to a minimum structural weight of 21.524 tons. Across 20 independent runs, the algorithm consistently achieved high-quality solutions, with a mean optimized weight of 22.476 tons, a worst-case result of 23.340 tons, and a relatively low standard deviation of 0.4623 tons. This indicates stable performance and reliable convergence toward near-optimal solutions with minimal variability between runs. Notably, all solutions fully satisfied the imposed design constraints, including stress, displacement, buckling, and slenderness limits, with no violations observed in any case.

No.	Design Variables	Section (mm^2)		No.	Design Variables	Section (mm^2)	
1	A_1	PIPE12XS	(12387.0725)	100	A_{100}	PIPE8Std	(5419.3438)
2	A_2	PIPE3XXS	(3529.0251)	101	A_{101}	PIPE2Std	(690.3212)
3	A_3	PIPE3-1/2Std	(1729.0288)	102	A_{102}	PIPE2-1/2Std	(1096.772)
4	A_4	PIPE8XXS	(13741.9075)	103	A_{103}	PIPE2-1/2XXS	(2599.9949)
5	A_5	PIPE3XS	(1948.3832)	104	A_{104}	PIPE2XXS	(1716.1257)

6	A_{6}	PIPE2XXS	(1716.1257)	105	A_{105}	PIPE4Std	(2045.1572)
7	A_{7}	PIPE5Std	(2774.1881)	106	A_{106}	PIPE4XXS	(5225.7962)
8	A_{8}	PIPE4XXS	(5225.7962)	107	A_{107}	PIPE1-1/2XS	(690.3212)
9	A_{9}	PIPE3-1/2Std	(1729.0288)	108	A_{108}	PIPE10Std	(7677.4038)
10	A_{10}	PIPE3-1/2Std	(1729.0288)	109	A_{109}	PIPE3Std	(1438.7068)
11	A_{11}	PIPE4Std	(2045.1572)	110	A_{110}	PIPE4XS	(2845.1555)
12	A_{12}	PIPE6Std	(3599.9928)	111	A_{111}	PIPE4XXS	(5225.7962)
13	A_{13}	PIPE4XS	(2845.1555)	112	A_{112}	PIPE3-1/2Std	(1729.0288)
14	A_{14}	PIPE4XS	(2845.1555)	113	A_{113}	PIPE5XS	(3941.9277)
15	A_{15}	PIPE2-1/2Std	(1096.772)	114	A_{114}	PIPE2-1/2Std	(1096.772)
16	A_{16}	PIPE4Std	(2045.1572)	115	A_{115}	PIPE4XXS	(5225.7962)
17	A_{17}	PIPE2-1/2XXS	(2599.9949)	116	A_{116}	PIPE10Std	(7677.4038)
18	A_{18}	PIPE5XS	(3941.9277)	117	A_{117}	PIPE2-1/2Std	(1096.772)
19	A_{19}	PIPE2XXS	(1716.1257)	118	A_{118}	PIPE3-1/2Std	(1729.0288)
20	A_{20}	PIPE2Std	(690.3212)	119	A_{119}	PIPE4XXS	(5225.7962)
21	A_{21}	PIPE6Std	(3599.9928)	120	A_{120}	PIPE2Std	(690.3212)
22	A_{22}	PIPE5XS	(3941.9277)	121	A_{121}	PIPE3XS	(1948.3832)
23	A_{23}	PIPE3XXS	(3529.0251)	122	A_{122}	PIPE3-1/2Std	(1729.0288)
24	A_{24}	PIPE4XS	(2845.1555)	123	A_{123}	PIPE1-1/2XS	(690.3212)
25	A_{25}	PIPE2XS	(954.8368)	124	A_{124}	PIPE8XS	(8258.0481)
26	A_{26}	PIPE8Std	(5419.3438)	125	A_{125}	PIPE5Std	(2774.1881)
27	A_{27}	PIPE3-1/2XS	(2374.1888)	126	A_{126}	PIPE2-1/2Std	(1096.772)
28	A_{28}	PIPE6XS	(5419.3438)	127	A_{127}	PIPE8XS	(8258.0481)
29	A_{29}	PIPE4XS	(2845.1555)	128	A_{128}	PIPE1-1/4XS	(568.3859)
30	A_{30}	PIPE2-1/2Std	(1096.772)	129	A_{129}	PIPE3-1/2Std	(1729.0288)
31	A_{31}	PIPE1-1/4Std	(431.6121)	130	A_{130}	PIPE3XS	(1948.3832)
32	A_{32}	PIPE6XXS	(10064.4962)	131	A_{131}	PIPE2-1/2Std	(1096.772)
33	A_{33}	PIPE8XXS	(13741.9075)	132	A_{132}	PIPE8Std	(5419.3438)
34	A_{34}	PIPE3-1/2Std	(1729.0288)	133	A_{133}	PIPE2XS	(954.8368)
35	A_{35}	PIPE10Std	(7677.4038)	134	A_{134}	PIPE2-1/2Std	(1096.772)
36	A_{36}	PIPE8XS	(8258.0481)	135	A_{135}	PIPE6XS	(5419.3438)
37	A_{37}	PIPE2Std	(690.3212)	136	A_{136}	PIPE1-1/2XS	(690.3212)
38	A_{38}	PIPE8XXS	(13741.9075)	137	A_{137}	PIPE1-1/4Std	(431.6121)
39	A_{39}	PIPE8XXS	(13741.9075)	138	A_{138}	PIPE2XXS	(1716.1257)
40	A_{40}	PIPE3Std	(1438.7068)	139	A_{139}	PIPE2Std	(690.3212)
41	A_{41}	PIPE5XXS	(7290.3081)	140	A_{140}	PIPE10Std	(7677.4038)
42	A_{42}	PIPE5XXS	(7290.3081)	141	A_{141}	PIPE3-1/2Std	(1729.0288)
43	A_{43}	PIPE6XS	(5419.3438)	142	A_{142}	PIPE4Std	(2045.1572)
44	A_{44}	PIPE4XXS	(5225.7962)	143	A_{143}	PIPE5XXS	(7290.3081)
45	A_{45}	PIPE4XXS	(5225.7962)	144	A_{144}	PIPE2-1/2Std	(1096.772)
46	A_{46}	PIPE6XS	(5419.3438)	145	A_{145}	PIPE2XS	(954.8368)
47	A_{47}	PIPE3-1/2Std	(1729.0288)	146	A_{146}	PIPE2XS	(954.8368)
48	A_{48}	PIPE4Std	(2045.1572)	147	A_{147}	PIPE3-1/2Std	(1729.0288)
49	A_{49}	PIPE6Std	(3599.9928)	148	A_{148}	PIPE5XS	(3941.9277)
50	A_{50}	PIPE5XS	(3941.9277)	149	A_{149}	PIPE1-1/2XS	(690.3212)
51	A_{51}	PIPE6Std	(3599.9928)	150	A_{150}	PIPE2-1/2Std	(1096.772)
52	A_{52}	PIPE8Std	(5419.3438)	151	A_{151}	PIPE3XXS	(3529.0251)
53	A_{53}	PIPE5Std	(2774.1881)	152	A_{152}	PIPE1-1/2XS	(690.3212)
54	A_{54}	PIPE4Std	(2045.1572)	153	A_{153}	PIPE1-1/4Std	(431.6121)
55	A_{55}	PIPE6Std	(3599.9928)	154	A_{154}	PIPE2Std	(690.3212)
56	A_{56}	PIPE5XS	(3941.9277)	155	A_{155}	PIPE2Std	(690.3212)
57	A_{57}	PIPE8Std	(5419.3438)	156	A_{156}	PIPE3XXS	(3529.0251)
58	A_{58}	PIPE4XS	(2845.1555)	157	A_{157}	PIPE5Std	(2774.1881)
59	A_{59}	PIPE3-1/2Std	(1729.0288)	158	A_{158}	PIPE2-1/2Std	(1096.772)
60	A_{60}	PIPE3-1/2Std	(1729.0288)	159	A_{159}	PIPE5XS	(3941.9277)
61	A_{61}	PIPE3XXS	(3529.0251)	160	A_{160}	PIPE1-1/2XS	(690.3212)
62	A_{62}	PIPE4XXS	(5225.7962)	161	A_{161}	PIPE2-1/2Std	(1096.772)
63	A_{63}	PIPE8Std	(5419.3438)	162	A_{162}	PIPE2Std	(690.3212)
64	A_{64}	PIPE3XXS	(3529.0251)	163	A_{163}	PIPE2-1/2XS	(1451.61)
65	A_{65}	PIPE3XS	(1948.3832)	164	A_{164}	PIPE4XS	(2845.1555)
66	A_{66}	PIPE3-1/2XS	(2374.1888)	165	A_{165}	PIPE1-1/2XS	(690.3212)
67	A_{67}	PIPE3-1/2XS	(2374.1888)	166	A_{166}	PIPE2-1/2Std	(1096.772)
68	A_{68}	PIPE3-1/2Std	(1729.0288)	167	A_{167}	PIPE2-1/2XXS	(2599.9949)
69	A_{69}	PIPE12Std	(9419.3362)	168	A_{168}	PIPE2Std	(690.3212)
70	A_{70}	PIPE3XS	(1948.3832)	169	A_{169}	PIPE3-1/2Std	(1729.0288)
71	A_{71}	PIPE3XS	(1948.3832)	170	A_{170}	PIPE1-1/2XS	(690.3212)
72	A_{72}	PIPE12Std	(9419.3362)	171	A_{171}	PIPE3-1/2Std	(1729.0288)
73	A_{73}	PIPE4XXS	(5225.7962)	172	A_{172}	PIPE5Std	(2774.1881)
74	A_{74}	PIPE8XS	(8258.0481)	173	A_{173}	PIPE3-1/2Std	(1729.0288)

75	A_{75}	PIPE5XXS	(7290.3081)	174	A_{174}	PIPE2-1/2Std	(1096.772)
76	A_{76}	PIPE8Std	(5419.3438)	175	A_{175}	PIPE2-1/2XXS	(2599.9949)
77	A_{77}	PIPE4XS	(2845.1555)	176	A_{176}	PIPE2Std	(690.3212)
78	A_{78}	PIPE10XS	(10387.0762)	177	A_{177}	PIPE2-1/2Std	(1096.772)
79	A_{79}	PIPE5XXS	(7290.3081)	178	A_{178}	PIPE2Std	(690.3212)
80	A_{80}	PIPE10Std	(7677.4038)	179	A_{179}	PIPE2-1/2Std	(1096.772)
81	A_{81}	PIPE8XXS	(13741.9075)	180	A_{180}	PIPE3-1/2Std	(1729.0288)
82	A_{82}	PIPE3Std	(1438.7068)	181	A_{181}	PIPE2Std	(690.3212)
83	A_{83}	PIPE8XXS	(13741.9075)	182	A_{182}	PIPE3-1/2Std	(1729.0288)
84	A_{84}	PIPE10Std	(7677.4038)	183	A_{183}	PIPE1-1/2XS	(690.3212)
85	A_{85}	PIPE8Std	(5419.3438)	184	A_{184}	PIPE1-1/2Std	(515.4829)
86	A_{86}	PIPE8XXS	(13741.9075)	185	A_{185}	PIPE1-1/2XS	(690.3212)
87	A_{87}	PIPE3-1/2Std	(1729.0288)	186	A_{186}	PIPE3Std	(1438.7068)
88	A_{88}	PIPE12XS	(12387.0725)	187	A_{187}	PIPE1-1/2Std	(515.4829)
89	A_{89}	PIPE6XS	(5419.3438)	188	A_{188}	PIPE2XS	(954.8368)
90	A_{90}	PIPE8XS	(8258.0481)	189	A_{189}	PIPE3Std	(1438.7068)
91	A_{91}	PIPE8XXS	(13741.9075)	190	A_{190}	PIPE2-1/2Std	(1096.772)
92	A_{92}	PIPE1Std	(318.709)	191	A_{191}	PIPE2XS	(954.8368)
93	A_{93}	PIPE5XXS	(7290.3081)	192	A_{192}	PIPE3-1/2Std	(1729.0288)
94	A_{94}	PIPE10Std	(7677.4038)	193	A_{193}	PIPE2-1/2Std	(1096.772)
95	A_{95}	PIPE5XS	(3941.9277)	194	A_{194}	PIPE2-1/2Std	(1096.772)
96	A_{96}	PIPE8Std	(5419.3438)	195	A_{195}	PIPE1-1/2Std	(515.4829)
97	A_{97}	PIPE3-1/2Std	(1729.0288)	196	A_{196}	PIPE1-1/2Std	(515.4829)
98	A_{98}	PIPE1-1/2XS	(690.3212)	197	A_{197}	PIPE4XXS	(5225.7962)
99	A_{99}	PIPE5XXS	(7290.3081)	198	A_{198}	PIPE4XXS	(5225.7962)

No.	Design Variables	Coordinates (mm)
199	X_1-X_2	**406.2288128**
200	X_5-X_6	**1236.764795**
201	X_9-X_{10}	**-1705.915486**
202	X_{13}-X_{14}	**-3624.131857**
203	X_{17}-X_{18}	**-4017.399393**
204	X_{21}-X_{22}	**-2735.13878**
205	X_{25}-X_{26}	**-628.7392905**
206	Z_{41}-Z_{42}	**19636.57685**
207	Z_{43}-Z_{44}	**20243.17519**
208	Z_{45}-Z_{46}	**20215.85988**
209	Z_{47}-Z_{48}	**20179.17627**
210	Z_{49}-Z_{50}	**20106.71417**
211	Z_{51}-Z_{52}	**20224.32589**
Weight (ton)		**21.524**
Constraint violation percentage (%)		**None**

Table 2: Optimum results for the 198-bar truss

The optimized configuration of the 198-bar truss is represented in Figure 2, with a colormap reflecting the stress capacity ratio of each element under the most unfavorable loading condition.

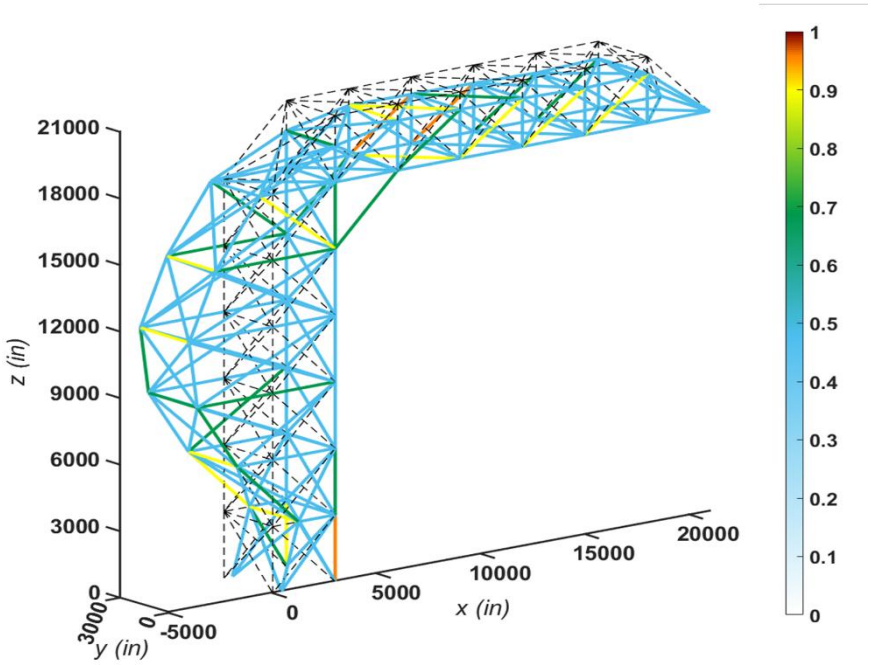

Figure 2: The optimized design of the 198-bar truss by CSBO with a colormap of stresses in members

Furthermore, the stress constraints for all structural members and the displacement limits for all nodes are maintained, showcased in Figures 3 and 4, respectively. Additionally, slenderness ratio constraints for all members are satisfied, as shown in Figure 5.

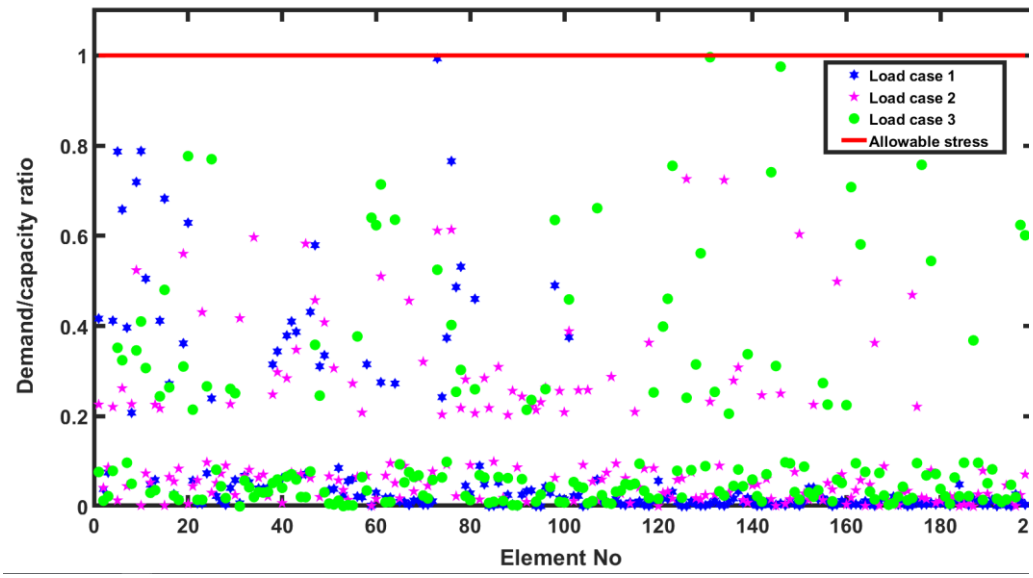

Figure 3: Comparison of member stresses with the allowable limit at the optimized design of the 198-bar truss.

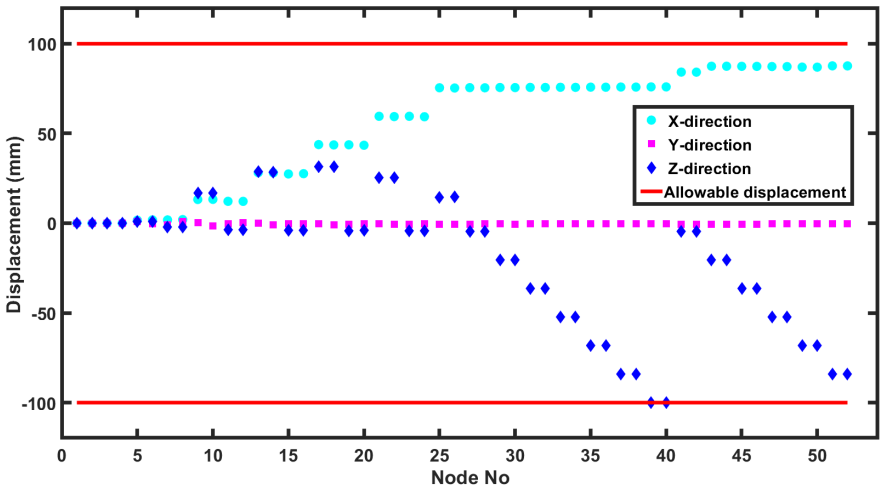

Figure 4: Comparison of nodal displacement with the allowable limit at the optimized design of the 198-bar truss.

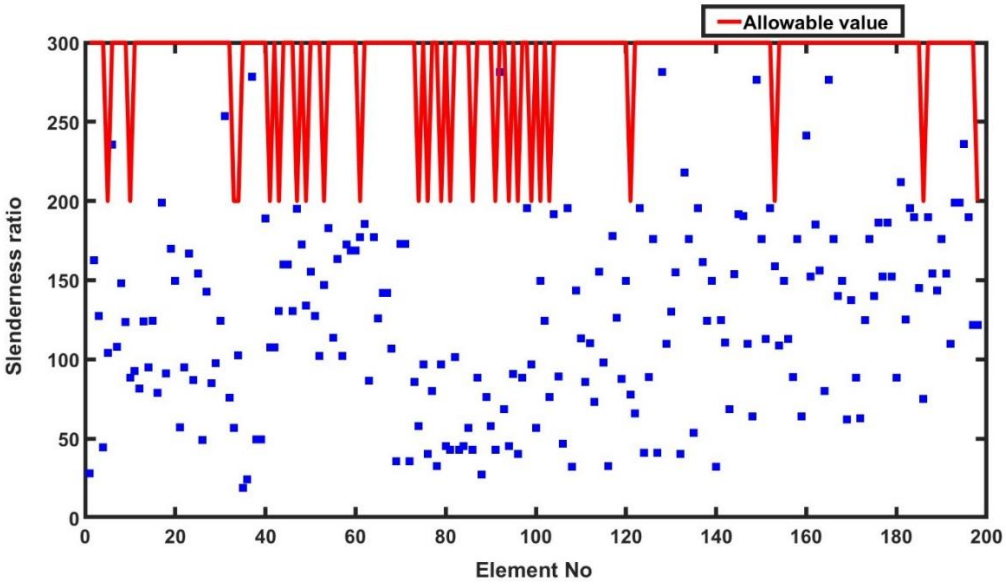

Figure 5: Comparison of member slenderness ratio with the allowable limit at the optimized design of the 198-bar truss.

The convergence curves depicting the relationship between the number of iterations and the optimal design across 20 separate runs, including the best-performing run, are

demonstrated in Figure 6. This convergence of the best run continues until the maximum iteration count of 2000 is reached.

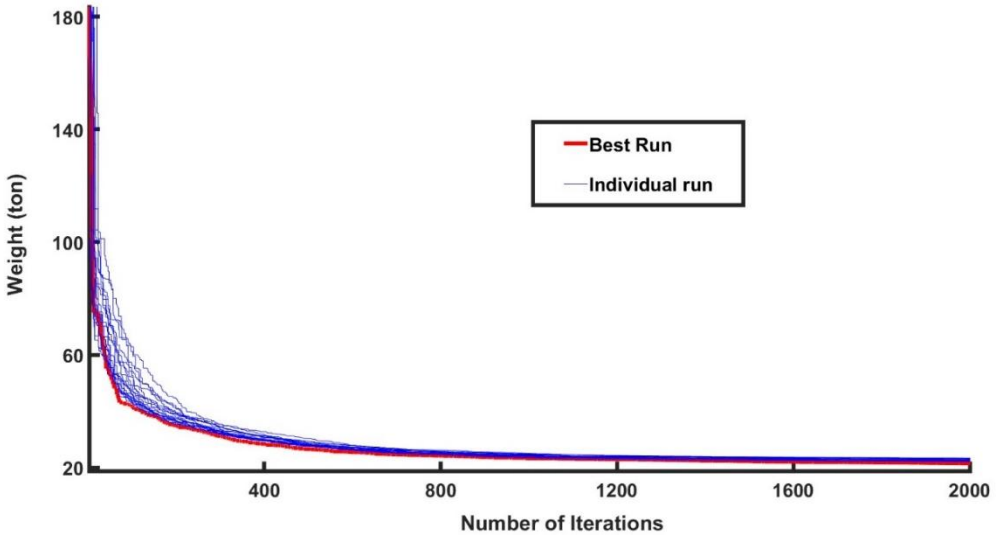

Figure 6: Comparison of member slenderness ratio with the allowable limit at the optimized design of the 198-bar truss.

The achieved optimal design is modeled within the globally recognized structural engineering software SAP2000 [19] for validation and cross-verification.. Furthermore, the design check tool of SAP2000 [19] is employed, confirming that all steel frames passed the stress/capacity check, as shown in Fig. 7. Due to the extensive nature of the analysis outcomes, which would significantly lengthen the paper, the detailed comparison between the self-developed MATLAB program and the commercial structural analysis software is not included here. The results highlight that the proposed algorithm not only demonstrates its potential as an alternative to SAP2000 but also offers an efficient solution for shape optimization, an aspect not readily available within SAP2000's capabilities.

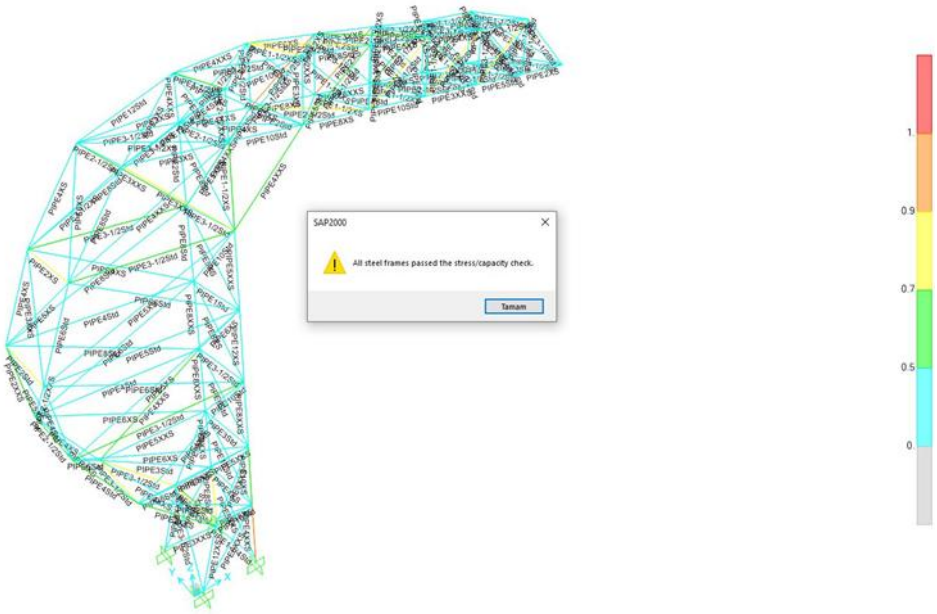

Figure 7: Stress/capacity check using SAP2000 software for the optimal design.

5 Concluding remarks

In this study, the standard Circulatory System-Based Optimization (CSBO) algorithm was successfully applied for the simultaneous sizing and shape optimization of a complex steel truss structure. A dedicated MATLAB-based program was developed to automate the optimization process, performing structural analysis and design checks that closely resemble the procedures used in SAP2000. Notably, the developed program extends beyond traditional workflows by incorporating shape optimization, which enables nodal coordinates to vary in tandem with member sizing, thereby providing a more comprehensive design approach. The optimization of a 3D spatial truss structure with 198 members and 211 design variables was conducted under the AISC-LRFD design specifications, considering stress, displacement, buckling, and slenderness constraints. The optimized results were validated through independent analysis in SAP2000 to confirm their accuracy and structural feasibility. Additionally, multiple independent optimization runs were performed to demonstrate the robustness and consistent convergence behaviour of the CSBO algorithm.

The results highlight the practical potential of CSBO for solving large-scale, high-dimensional structural optimization problems and demonstrate that the developed optimization framework can serve as an effective tool for advanced truss design applications in structural engineering.

References

[1] Goldberg DE (1989) Genetic Algorithms in Search, Optimization, and Machine Learning, Addison-Wesley, Reading, MA, 1989. NN Schraudolph J. 3

[2] Kirkpatrick S, Gelatt Cd, Vecchi Mp (1983) Optimization By Simulated Annealing. Science (80-) 220:671–680.

[3] Kennedy J, Eberhart R (1995) Particle swarm optimization. In: IEEE International Conference on Neural Networks - Conference Proceedings

[4] Geem ZW, Kim JH, Loganathan G V (2001) A new heuristic optimization algorithm: Harmony search. Simulation 76:60–68.

[5] Erol OK, Eksin I (2006) A new optimization method: Big Bang Big Crunch. Adv Eng Softw 37:106–111.

[6] Dorigo M, Maniezzo V, Colorni A (1996) Ant system: Optimization by a colony of cooperating agents. IEEE Trans Syst MAN Cybern Part B-Cybernetics 26:29–41.

[7] Karaboga D, Basturk B (2007) A powerful and efficient algorithm for numerical function optimization: Artificial bee colony (ABC) algorithm. J Glob Optim 39:.

[8] Storn, R., & Price, K. (1997). Differential evolution–a simple and efficient heuristic for global optimization over continuous spaces. *Journal of global optimization*, *11*, 341-359.

[9] Zhao S, Zhang T, Ma S, Chen M (2022) Dandelion Optimizer: A nature-inspired metaheuristic algorithm for engineering applications. Eng Appl Artif Intell 114.

[10] S. Mirjalili, S. M. Mirjalili, and A. Lewis, "Grey Wolf Optimizer," *Advances in Engineering Software*, vol. 69, pp. 46–61, 2014,

[11] M. B. Ali and A. A. Heidari, (2022) "Bonobo Optimizer: A New Meta-Heuristic Algorithm for Solving Engineering Optimization Problems," *Engineering Computations*, vol. 39, no. 4, pp. 1345–1381.

[12] Ghasemi M, Akbari MA, Jun C, et al (2022) Circulatory System Based Optimization (CSBO): an expert multilevel biologically inspired meta-heuristic algorithm. Eng. Appl. Comput. Fluid Mech. 16

[13] Lamberti L, Pappalettere C (2010) Metaheuristic Design Optimization of Skeletal Structures: A Review. Comput Technol Rev 4:. https://doi.org/10.4203/ctr.4.1

[14] Eid HF, Garcia-Hernandez L, Abraham A (2022) Spiral water cycle algorithm for solving multi-objective optimization and truss optimization problems. Eng Comput 38:.

[15] Grzywiński M, Selejdak J, Dede T (2019) Shape and size optimization of trusses with dynamic constraints using a metaheuristic algorithm. Steel Compos Struct 33:.

[16] Azizi M, Baghalzadeh Shishehgarkhaneh M, Basiri M (2022) Optimum design of truss structures by Material Generation Algorithm with discrete variables. Decis Anal J 3

[17] Degertekin SO, Minooei M, Santoro L, et al (2021) Large-scale truss-sizing optimization with enhanced hybrid hs algorithm. Appl Sci 11

[18] AISC-LRFD (2001) Manual of steel construction-Load and Resistance Factor Design. Am Inst Steel Constr

[19] Computers & Structures Inc (2019) Sap 2000. Sap 2000

[20] Bright Optimizer International Student Competition in Structural Optimization. www.brightoptimizer.com